Supplementary Information

Highly active cocatalyst-free semiconductor photocatalyst for visible-light-driven hydrogen evolution: synergistic effect of surface defects and spatial bandgap engineering

Guiyang Yu,[a] Wenxiang Zhang,[a] Yanjun Sun,[a] Tengfeng Xie,[a] Ai-Min Ren,[c] Xin Zhou*[b] and Gang Liu*[a]

[a] Key Laboratory of Surface and Interface Chemistry of Jilin Province, College of Chemistry, Jilin University, Jiefang Road 2519, Changchun, 130012, China. *E-mail: lgang@jlu.edu.cn

[b] College of Environment and Chemical Engineering, Dalian University, Dalian, 116622, China. E-mail: zhouxin@dlu.edu.cn

[c] Institute of Theoretical Chemistry, Jilin University, Changchun, 130012, China.

Experimental Section

Photocatalysts preparation.

All chemicals used in the experiments were of analytical grade, and were used without further purification. Double-distilled water was used in all of the experiments. $Zn_{1-x}Cd_xS/SiO_2$ is a composite of sulfide semiconductor dispersed on mesoporous silica, which was prepared by a two-step method. This method was reported recently by our group on the preparation of supported CdS catalysts.[S1] In the first step, the precursor $Zn_{1-x}Cd_xO/SiO_2$ was prepared by a sol-gel method in the presence of citric acid. Typically, 20 mL tetraethyl orthosilicate (TEOS) was added into an 7.5 mL aqueous solution containing 1.092 g $Zn(NO_3)_2$, 0.566 g $Cd(NO_3)_2$ and 4.3 g citric acid. Then, an aqueous HNO_3 solution (2 $mol \cdot L^{-1}$) was used to adjust the pH value of the solution to 2.0. After standing for 0.5 h, the mixture was heated at 80 °C in open air to remove water and all other volatiles. After that, the dried solid was calcined at 600 °C for 3 h (heating rate is 10 $K \cdot min^{-1}$) to obtain the $Zn_{1-x}Cd_xO/SiO_2$. The weight percent of $Zn_{1-x}Cd_xO$ in $Zn_{1-x}Cd_xO/SiO_2$ is 15%. The stoichiometric molar ratio of Cd:Zn is 0.367:1 and the sample could be recorded as $Zn_{0.67}Cd_{0.33}O/SiO_2$.

In the second step, $Zn_{1-x}Cd_xO/SiO_2$ was sulfurized in a Na_2S aqueous solution. Typically, 0.5 g of $Zn_{1-x}Cd_xO/SiO_2$ was sonicated in 20 mL distilled water. Then, 15 mL 0.05 M Na_2S solution was added dropwise to the above mixture of $Zn_{1-x}Cd_xO/SiO_2$ with magnetic stirring at room temperature. After stirring for another 12 h, $Zn_{1-x}Cd_xS/SiO_2$ formed in the suspension was filtered and washed with distilled water to remove non-reacted reactants (S^{2-}). After that, the products were fully dried at 80ºC in an oven to obtain the final $Zn_{1-x}Cd_xS/SiO_2$. For comparison, pure CdS/SiO_2 and ZnS/SiO_2 was prepared with the same procedure as described above without the addition of $Zn(NO_3)_2$ or $Cd(NO_3)_2$.

Pure $Zn_{0.67}Cd_{0.33}S$ solid solution possessing cubic structure was prepared by co-precipitation method.[S2] Na_2S aqueous solution (0.05M, 110 mL) was added dropwise to an aqueous solution (30 mL) containing 1.638 g $Zn(NO_3)_2$ and 0.566 g $Cd(NO_3)_2$ with magnetic stirring at room temperature. After stirring for another 12 h, the product

was filtered and washed with deionized water several times, and dried at 80 ºC in an oven.

The hexagonal wurtzite $Zn_{0.67}Cd_{0.33}S$ solid solution was prepared by hydrothermal method.[S3] Typically, 100 mL *L*-cysteine solution (50 mM) was mixed with $Zn(NO_3)_2$ and $Cd(NO_3)_2$ aqueous solution. The stoichiometric molar ratio of *L*-cysteine to $Zn(NO_3)_2$ and $Cd(NO_3)_2$ is 2:1. The mixture was stirred for 30 min to form the stable complexes of cysteine-(Cd^{2+}-Zn^{2+}). Then a total volume of 50 mL deionized water was added to the above mixture and transferred to 40 mL Teflon-lined stainless-steel autocalves. The autoclaves were maintained at 130 °C for 6 h and then cooled to room temperature naturally. The products were filtered and washed with distilled water to remove remaining ions and impurities. After that, the products were fully dried at 80 °C in an oven to obtain the final product.

Materials Characterizations.

Powder X-ray diffraction (XRD) patterns were recorded on a Rigaku X-ray diffractometer using CuKα radiation (λ=1.5418 Å). UV-vis diffused reflectance spectra of the samples were obtained from UV-vis-NIR spectrophotometer (Shimadzu-3600). N_2 adsorption-desorption isotherms were measured at 77 K, using a Micromeritics ASAP 2010N analyzer. Samples were degassed at 423 K for 20 h before measurements. Specific surface areas were calculated using the Brunauer-Emmett-Teller (BET) model. Pore size distributions were evaluated from adsorption branches of nitrogen isotherms using the Barret-Joyner-Halenda (BJH) model. Transmission electron microscopy (TEM) images were taken with a JEM-2100F with an accelerating voltage of 200 kV equipped with an energy-dispersive spectroscopy analyzer. The photoluminescence (PL) measurement was carried out on the FLS920 (Edinburgh Instrument) at room temperature using the excitation wavelength of 390 nm. The SPV spectra measurements were carried out based on a lock-in amplifier. The measurement system consisted of a light source from a 532 nm continuous laser, a lock-in amplifier (SR830, Stanford Research Systems, Inc.) and a sample chamber. The continuous laser light was modulated with a chopper (SR540, Stanford Research Systems, Inc.). The frequency

dependent SPV is generated when the sample is excited by periodic light with different modulation frequencies. The SPV transient measurement system consisted of laser pulse radiation (pulse width, 5 ns) from a Nd:YAG laser (Polaris II, New Wave Research, Inc.), a 500 MHz digital phosphor oscilloscope (TDS 5054, Tektronix) with a preamplifier and a sample chamber. XPS was performed on a Thermo ESCA LAB 250 system with MgKα source (1254.6 eV), where Ar^+ bombardment was performed and surface chemical state of the sample was characterized. The binding energies were calibrated using C 1s peak at 284.6 eV as standard. X-ray source with the take-off angle of 90º after different Ar^+ bombardment time. The energy resolution of the instrument at 20eV of pass energy is 0.6eV, as estimated from the full width at half maximum (FWHM) of Ag $3d_{5/2}$ peak. The Ar^+ bombardment was operated with EX05 argon ion gun whose angle arrangement given the sample surface normal is 45^0 at a chamber pressure of 1×10^{-6} Pa. The ion beam voltage was 3 kV and the emission current was 2 μA. The etching area was 2 mm × 2 mm, which was much larger than X-ray spot (500 μm in diameter).

Photocatalytic Reaction.

The photocatalytic H_2 evolution reactions were carried out in a flowing gas diffluent system. The catalyst powder (0.1 g) was dispersed by a magnetic stirrer in 100 mL of 0.35 M Na_2S and 0.25 M Na_2SO_3 aqueous solution in a reaction cell made of Pyrex glass. The reaction temperature was maintained at 15 °C. The reaction solution was evacuated 30 min to ensure complete air removal prior to light irradiation. Magnetic stirring was used to keep the photocatalyst particles in a suspension state. A 300 W Xe-lamp with a cutoff filter was employed for visible-light ($\lambda \geq 420$nm) irradiation. The amounts of evolved H_2 was determined by an online gas chromatograph (GC122, TCD) equipped with a 4 m 5 A molecular sieve columns and Ar as gas.

The apparent quantum yield was measured under the same photocatalytic reaction except for the wavelength of irradiation light. The apparent quantum yields of 0.1 g photocatalysts in one continuous reaction under visible light with different wavelengths of 420, 450, 500, 550, 600 nm were measured. Apparent quantum yields at different

wavelengths were calculated by the following function. The band-pass and cutoff filters and a photodiode were used in measurement.

$$\mathrm{AQY}(\%) = \frac{\text{Number of reacted electrons}}{\text{Total number of incident photons}} \times 100$$
$$= \frac{2 \times \text{The number of evoluted } H_2 \text{ molecules}}{\text{Total number of incident photons}} \times 100$$

Computational Method

All the calculations were performed with the Vienna ab initio simulation package [S4,S5] and projector augmented wave method.[S6,S7] The wave function was expanded by plane wave with kinetic cutoff of 400 eV. The generalized gradient approximation (GGA) with the spin-polarized Perdew−Burke−Ernzerhof (PBE) functional[S8] was used for all of the calculations. For bulk cubic ZnS, the calculated lattice parameter, *a* = 5.445 Å is in good agreement with experimental value.[S9, S10] A 2×2×2 supercell including 64 atoms was used to simulate $Zn_{1-x}Cd_xS$ solid solution. A 3×3×3 Monkorst-Pack k-point mesh was applied on structural and energy calculations. On top of optimized geometries obtained at the GGA-PBE level, a more accurate approach,[S11-S13] the hybrid HSE06 functional, was used to calculate electronic properties.

Based on the results of the band gap calculations, the conduction band edge energy (E_c) for the $Zn_{1-x}Cd_xS$ solid solution was computed using the method developed by Butler and Ginley:[S12,S13]

$$E_c = E_0 - \chi + 1/2 \times E_g \qquad (1)$$

$$\chi_{[Zn1\text{-}xCdxS]} = (\chi_{Zn}^{1-x} \times \chi_{Cd}^{x} \times \chi_{S}^{1})^{1/2} \qquad (2)$$

$$\chi_M = 1/2 \times (A_f + I_1) \qquad (3)$$

where E_0 is a consistent relating the reference electrode to the vacuum level, and E_0 = 4.50 eV for the standard hydrogen electrode; E_g is the semiconductor band gap; χ is the geometric mean of the Mulliken electronegativities of semiconductor constituents; Mulliken's definition of the electronegativity of a neutral atom is the arithmetic mean of the atomic electron affinity (A_f) and the first ionization energy (I_1). For S atom, the atomic electron affinity is 2.08 eV and the ionization potential is 10.36 eV. We cannot

use Eq. (3) to determine the atomic electronegativity of Cd and Zn, because atomic electron affinities for Cd and Zn are unknown. Considering that the electronegativity is identical to the work function of a metal,[S15] χ_{Zn} and χ_{Cd} can be replaced by the work function of Zn (3.63 eV) and Cd (4.08 eV), respectively.[S16,S17]

To compare the adsorption ability of hydrogen on different cubic CdS surfaces, we constructed both Cd-terminated and S-terminated CdS(100) surface using a slab model consisting of ten atomic layers. The top half of slab and the adsorbed H atom are allowed to fully relax and the bottom half of slab is held fixed. The slabs are set by a 13 Å vacuum layer. The Monkhorst-Pack scheme was used for *k*-point with a $5 \times 5 \times 1$ sampling grid. Structures were relaxed until all forces on atoms were less than 0.01 eV/Å.

Table S1. The surface atom contents of Zn, Cd, and S elements on $Zn_{1-x}Cd_xS/SiO_2$.

Ar^+ bombardment time (s)	**Cd content (at%)**	**Zn content (at%)**	**S content (at%)**	**S/(Cd+Zn) ratio in $Zn_{1-x}Cd_xS/SiO_2$**
0	1.59	3.25	3.51	0.725
60	1.33	3.17	3.23	0.718
120	1.21	3.15	3.20	0.734
180	0.94	2.94	2.75	0.708
240	0.75	2.46	2.27	0.707

Table S2. Cd/Zn ratio within $Zn_{1-x}Cd_xO/SiO_2$ and $Zn_{1-x}Cd_xS/SiO_2$ under different Ar^+ bombardment time.

Bombardment Time (s)	**Cd/Zn ratio within $Zn_{1-x}Cd_xO/SiO_2$**	**Cd/Zn ratio within $Zn_{1-x}Cd_xS/SiO_2$**
0	0.359:1	0.490:1
60	0.382:1	0.420:1
120	0.401:1	0.384:1
180	0.470:1	0.320:1
240	0.512:1	0.305:1

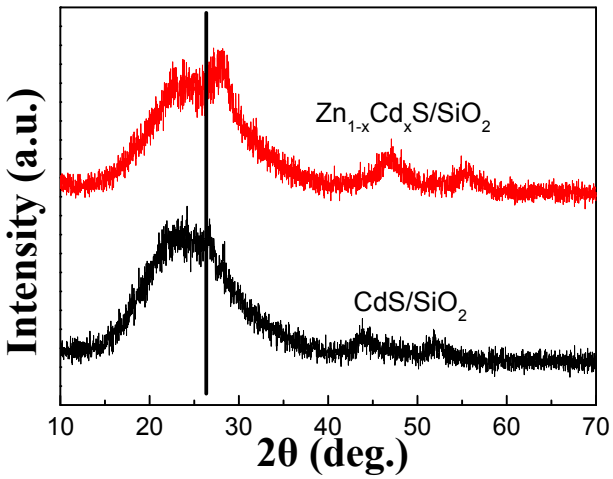

Fig. S1 XRD patterns of $Zn_{1-x}Cd_xS/SiO_2$ and CdS/SiO_2 samples.

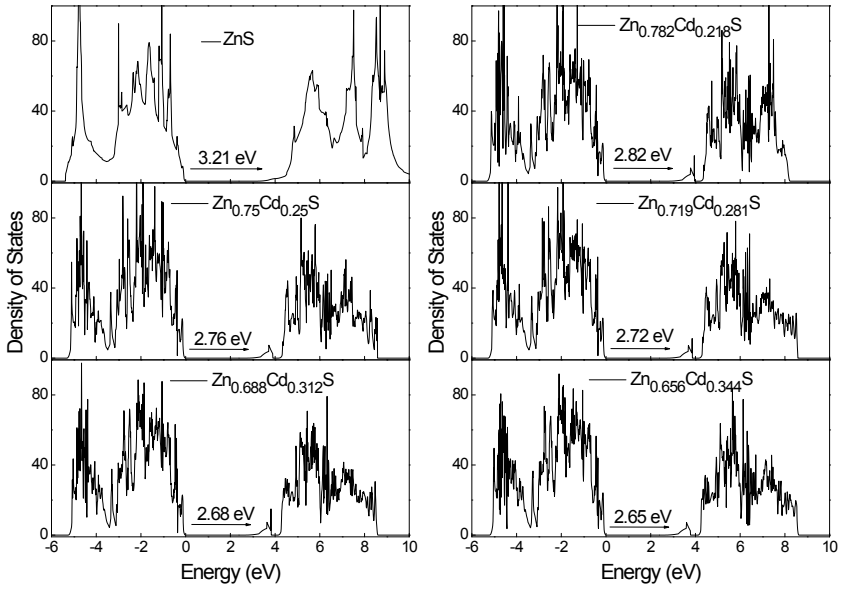

Fig. S2 Density of states for $Zn_{1-x}Cd_xS$.

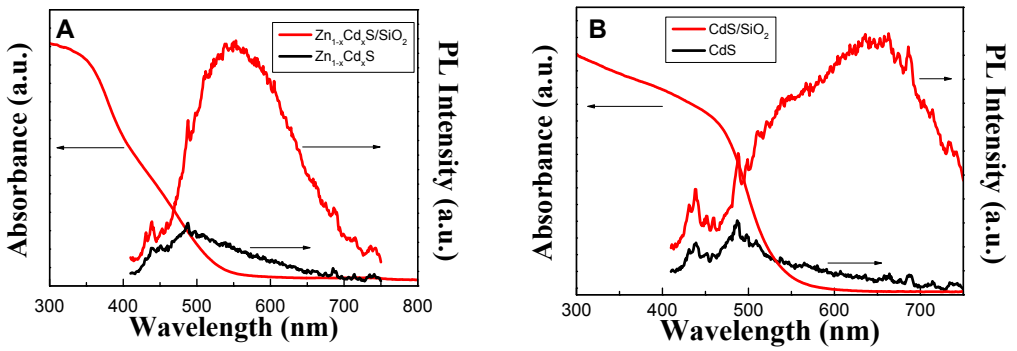

Fig. S3 UV-vis diffuse reflection and PL spectra of (A) $Zn_{1-x}Cd_xS/SiO_2$ and bulk $Zn_{1-x}Cd_xS$, (B) CdS/SiO_2 and bulk CdS.

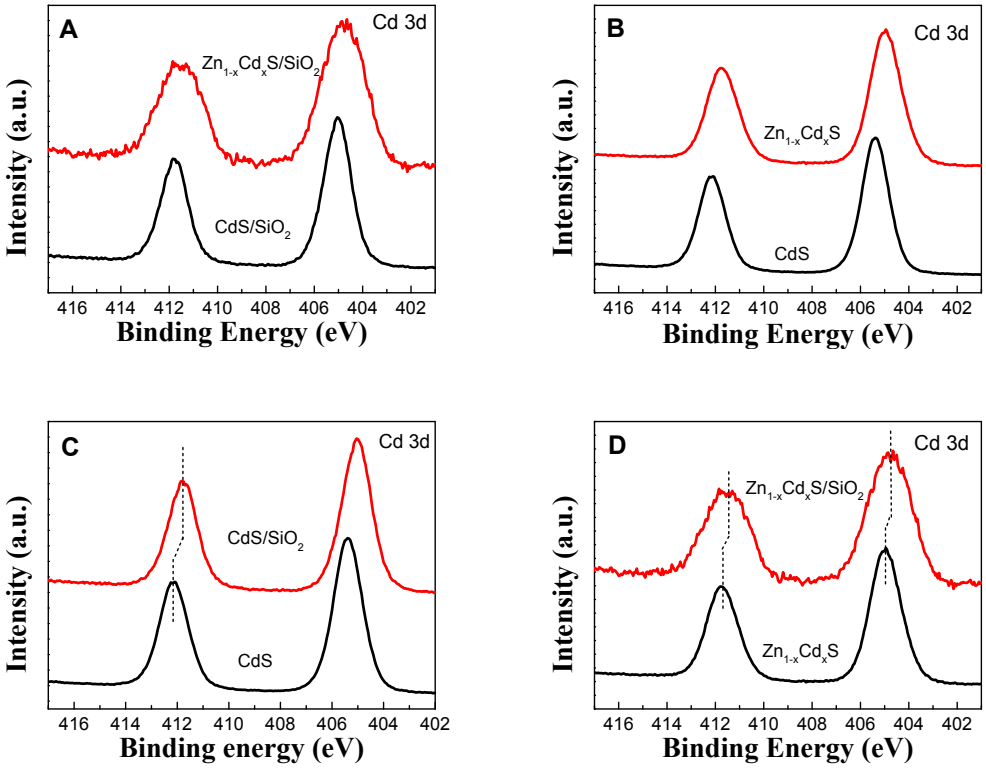

Fig. S4 Cd 3d XPS spectra of (A) CdS/SiO_2 and $Zn_{1-x}Cd_xS/SiO_2$, (B) CdS and $Zn_{1-x}Cd_xS$, (C) CdS and CdS/ SiO_2, (D) $Zn_{1-x}Cd_xS$ and $Zn_{1-x}Cd_xS/SiO_2$.

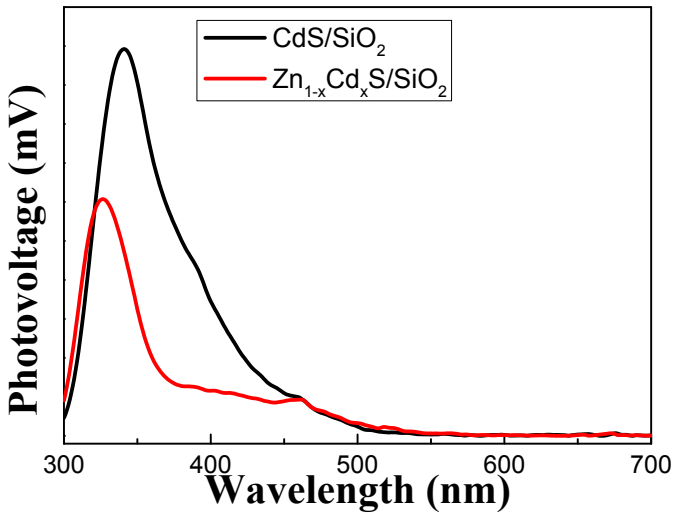

Fig. S5 SPV spectra of CdS/SiO_2 and $Zn_{1-x}Cd_xS/SiO_2$ samples.

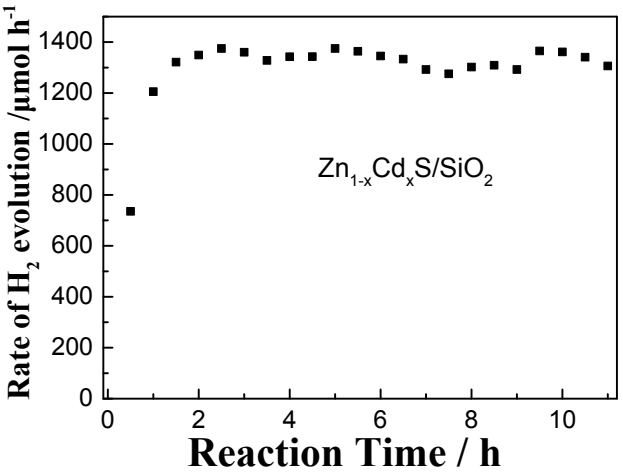

Fig. S6 Typical time course for H_2 production over $Zn_{1-x}Cd_xS/SiO_2$ under visible light irradiation. Reaction condition: 0.1 g photocatalysts in 100 mL Na_2S (0.35 M)-Na_2SO_3 (0.25 M) solution, 300 W Xe-lamp equipped with cut-off filter ($\lambda \geq 420$ nm).

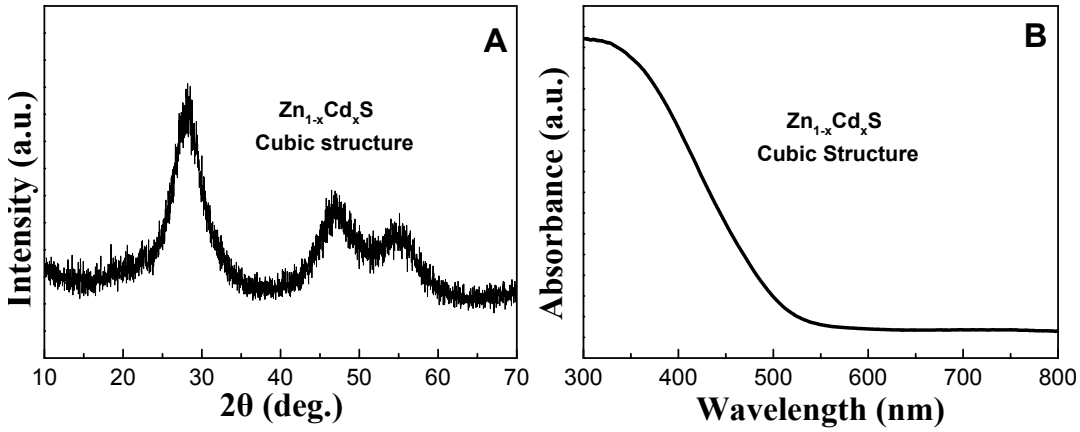

Fig. S7 (A) XRD pattern and (B) UV-vis diffuse reflection spectrum of cubic $Zn_{1-x}Cd_xS$ solid solution.

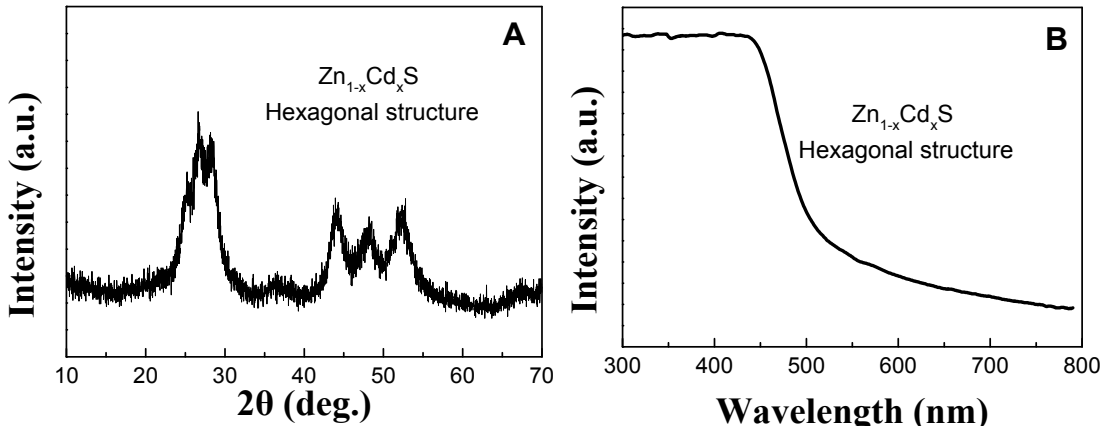

Fig. S8 (A) XRD pattern and (B) UV-vis diffuse reflection spectrum of hexagonal $Zn_{1-x}Cd_xS$ solid solution.

Table S3. Typical $Zn_{1-x}Cd_xS$ solid solution photocatalysts for hydrogen evolution with SO_3^{2-} and S^{2-} as sacrificial reagent.

Photocatalyst	Crystal structure	Preparation method	Cocatalyst	Light source	H_2 evolution rate ($\mu mol \cdot h^{-1} \cdot g^{-1}$)[a]	QY (%)[b]	Reference
$Zn_{0.67}Cd_{0.33}S/SiO_2$	Cubic structure	Sol-gel and anion exchange method	—	λ≥420nm (300W Xe lamp)	76228[c]	48.6 (420 nm)	Current work
$Zn_{0.67}Cd_{0.33}S$	Hexagonal wurtzite	Co-precipitation	—	λ≥420nm (300W Xe lamp)	5604	—	Current work for comparation
$Zn_{0.67}Cd_{0.33}S$	Cubic structure	Hydrothermal method	—	λ≥420nm (300W Xe lamp)	7250	—	Current work for comparation
$Zn_{0.5}Cd_{0.5}S$	Cubic structure	Precipitation-hydrothermal	—	λ≥400nm (300W Xe lamp)	17900	43.0 (425nm)	Energy Environ. Sci. 2011, 4, 1372-1378.
$Zn_{0.5}Cd_{0.5}S$	Hexagonal structure	Co-precipitation	—	λ≥400nm (350W Xe lamp)	7240	9.6 (420 nm)	ACS Catal. 2013, 3, 882-889
$Zn_{0.5}Cd_{0.5}S$	Hexagonal structure	Hydrothermal method	—	λ≥420nm (300W Xe lamp)	11420	16.9(420 nm)	Small, 2016, 12, 793-801
$Zn_{0.8}Cd_{0.2}S$	Cubic structure	Deposition-precipitation	0.25% Pt	λ≥420nm (300W Xe lamp)	3200	—	Nanoscale, 2012, 4, 2046-2053
$Zn_{0.3}Cd_{0.7}S$	Hexagonal structure	Co-precipitation	—	λ≥420nm (300W Xe lamp)	3500	—	Catal. Today, 2009, 143, 51-56

Table S3. Continued

Photocatalyst	Crystal structure	Preparation method	Cocatalyst	Light source	H_2 evolution rate ($\mu mol \cdot h^{-1} \cdot g^{-1}$)[a]	QY (%)[b]	Reference
$Zn_{0.56}Cd_{0.44}S$	Cubic structure	Co-precipitation	—	λ≥420nm (500W Xe lamp)	2640	—	Int. J. Hydrogen Energy 2010, 35, 19-25
$Zn_{0.16}Cd_{0.84}S$	Hexagonal structure	Co-precipitation	—	300W Xe lamp	16320	2.17	Int. J. Hydrogen Energy 2006, 31, 2018-2024
$Zn_{0.8}Cd_{0.2}S$	Hexagonal structure	Hydrothermal method	—	420nm≤λ≤780nm (300W Xe lamp)	3430	16.2(420 nm)	J. Colloid Interface Sci. 2016, 467, 97-104
$Zn_{0.5}Cd_{0.5}S$	Hexagonal structure	Co-precipitation	—	150W Xe lamp	2000	—	Ind. Eng. Chem. Res. 2010, 49, 6854-6861
$Zn_{0.5}Cd_{0.5}S$	Cubic structure	Co-precipitation	—	300W Hg lamp	1019	1.29(420 nm)	Int. J. Hydrogen Energy 2014, 39, 1630-1639
$Zn_{0.17}Cd_{0.83}S$	Cubic structure	Hydrothermal method	1% Pt	λ≥400nm (350W Xe lamp)	2128	6.3 (420 nm)	Chem. Commun. 2010, 12, 1611-1614
$Cu_{1.94}S$-$Zn_{0.77}Cd_{0.23}S$	Hexagonal structure	Colloid deposition method	5% Pt	λ≥420nm (300W Xe lamp)	13533	26.4 (420 nm)	J. Am. Chem. Soc. 2016, 138, 4286-4289
RGO-$Zn_{0.8}Cd_{0.2}S$	Cubic structure	Hydrothermal method	—	Solar-simulator (100mW/cm^2)	1824	23.4(420 nm)	Nano Lett. 2012, 12, 4584-4589

Table S3. Continued

Photocatalyst	Crystal structure	Preparation method	Cocatalyst	Light source	H_2 evolution rate ($\mu mol \cdot h^{-1} \cdot g^{-1}$)[a]	QY (%)[b]	Reference
CuS-$Zn_{0.17}Cd_{0.83}S$	x =0.83	Co-precipitation	1% Pt	λ≥420nm (300W Xe lamp)	2463	19.1(420 nm)	Int. J. Hydrogen Energy 2009, 34, 8495-8503
$Zn_{0.17}Cd_{0.83}S$-gC_3N_4	Zinc blend and wurtzite structure	Hydrothermal method	—	λ≥420nm (300W Xe lamp)	—	37(420 nm)	Int. J. Hydrogen Energy 2015, 40, 7546-7552

[a] H_2 evolution rate calculated based on the optimized activity in the corresponding literature.

[b] Quantum yield.

[c] H_2 evolution rate calculated based on the contents of $Zn_{0.67}Cd_{0.33}S$ in the $Zn_{0.67}Cd_{0.33}S/SiO_2$.

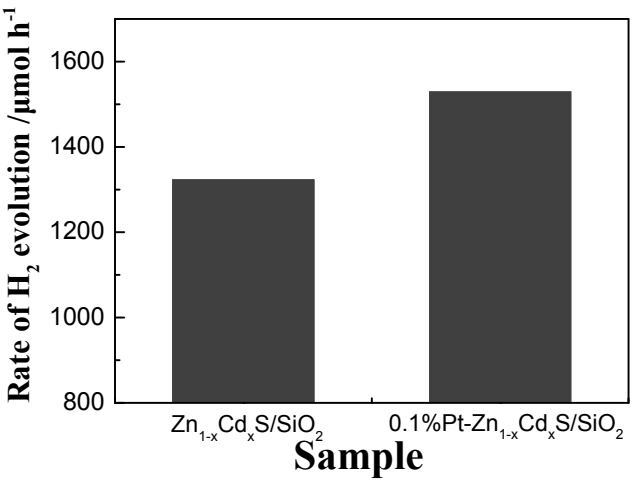

Fig. S9 Photocatalytic H_2 evolution activity of $Zn_{1-x}Cd_xS/SiO_2$, and 0.1%Pt-$Zn_{1-x}Cd_xS/SiO_2$ under visible light irradiation. Reaction condition: 0.1 g photocatalysts in 100 mL Na_2S (0.35 M)-Na_2SO_3 (0.25 M) solution, 300 W Xe-lamp equipped with cut-off filter ($\lambda \geq 420$ nm).

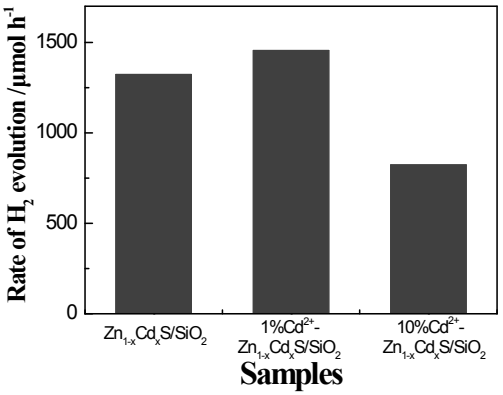

Fig. S10 Photocatalytic H_2 evolution activity of 1%Cd^{2+}-$Zn_{1-x}Cd_xS/SiO_2$, 10%Cd^{2+}-$Zn_{1-x}Cd_xS/SiO_2$, and $Zn_{1-x}Cd_xS/SiO_2$ under visible light irradiation. Cd^{2+} ions were loaded by impregnation method. Reaction condition: 0.1 g photocatalysts in 100 mL Na_2S (0.35 M)-Na_2SO_3 (0.25 M) solution, 300 W Xe-lamp equipped with cut-off filter ($\lambda \geq 420$ nm);

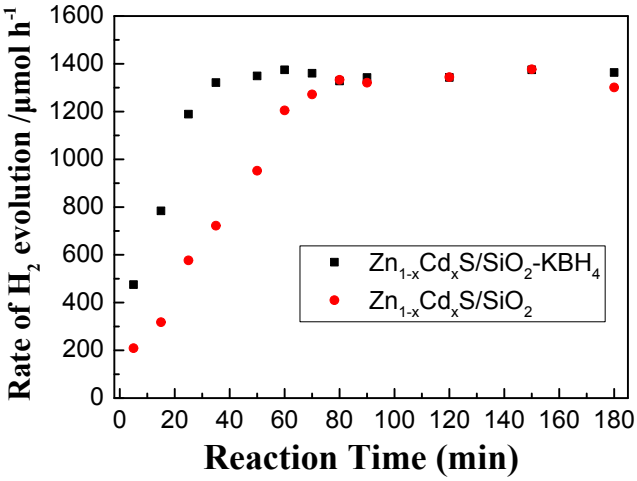

Fig. S11 Typical time course for H_2 production over $Zn_{1-x}Cd_xS/SiO_2$ and $Zn_{1-x}Cd_xS/SiO_2$ treated with 0.5 M KBH_4 solution under visible light irradiation. Reaction condition: 0.1 g photocatalysts in 100 mL Na_2S (0.35 M)-Na_2SO_3 (0.25 M) solution, 300 W Xe-lamp equipped with cut-off filter ($\lambda \geq 420$ nm).

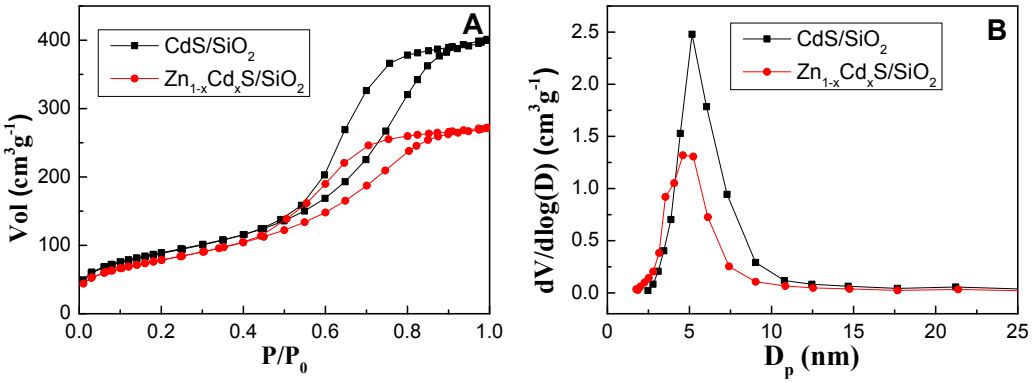

Fig. S12 N_2 adsorption-desorption isotherms and BJH pore size distribution of $Zn_{1-x}Cd_xS/SiO_2$ and CdS/SiO_2.

Table S4. Texture properties of CdS/SiO_2 and $Zn_{1-x}Cd_xS/SiO_2$ samples.

Sample	S_{BET} (m^2g^{-1})	Pore vol (cm^3g^{-1})	Pore size[a] (nm)
CdS/SiO_2	404	0.56	7.9
$Zn_{1-x}Cd_xS/SiO_2$	360	0.41	5.3

[a] Average pore diameters were calculated from adsorption branches using BJH model.

References:

[S1] G. Yu, L. Geng, S. Wu, W. Yan and G. Liu, *Chem. Commun.* 2015, **51**, 10676-10679.

[S2] M. Liu, L. Wang, G. Lu, X. Yao and L. Guo, *Energy Environ. Sci.* 2011, **4**, 1372-1378.

[S3] X. Ji, X. Song, J. Li, Y. Bai, W. Yang and X. Peng, *J. Am. Chem. Soc.* 2007, **129**, 13939.

[S4] G. Kesse and J. Furthmüller, *Phys. Rev. B* 1996, **54**, 11169-11186.

[S5] G. Kesse and J. Furthmüller, *Comput. Mater. Sci.* 1996, **6**, 15-50.

[S6] P. Blöchk, *Phys. Rev. B* 1994*,* **50**, 17953-17979.

[S7] G. Kresse and D. Joubert, *Phys. Rev. B* 1999, **59**, 1758-1775.

[S8] J. P. Predew, K. Burke and M. Ernzerhof, *Phys. Rev. Lett.* 1996, **77**, 3865-3868.

[S9] D. H. Wang, L. Wang and A. W. Xu, *Nanoscale* 2012, **4**, 2046-2053.

[S10] L. Wang, W. Wang, M. Shang, W. Yin, S. Sun and L. Zhang, *Int. J. Hydrogen Energy* 2010, **35**, 19-25.

[S11] J. Heyd, G. E. Scuseria and M. Ernzerhof, *J. Chem. Phys.* 2003, **118**, 8207-8215.

[S12] J. Heyd, G. E. Scuseria and M. Ernzerhof, *J. Chem. Phys.* 2004, **121**, 1187-1192.

[S13] J. Heyd, G. E. Scuseria and M. Ernzerhof, *J. Chem. Phys.* 2006, **124,** 219906.

[S14] M. A. Butler and D. S. Ginley, *J. Electrochem. Soc.* 1978, **125**, 228-232.

[S15] D. S. Ginley and M. A. Butler, *J. Electrochem. Soc.* 1978, **125**, 1968-1974.

[S16] J. M. Yuk, K. Kim, Z. Lee, M. Watanabe, A. Zettl, T. W. Kim, T. W. Kim, Y. S. No, W. K. Choi and J. Y. Lee, *ACS Nano*, 2010, **4**, 2999-3004.

[S17] J.-F. Salinas, J.-L. Maldonado, G. Ramos-Ortiz, M. Rodriguez, M.-A. Meneses-Nava, O. Barbosa-Garcia, R. Santillan and N. Farfán, *Sol. Energy Mater. Sol. Cells,* 2011, **95**, 595-601.